Probing Stellar Evolution and Fundamental Symmetries via Indirect Methods: The Trojan Horse Approach

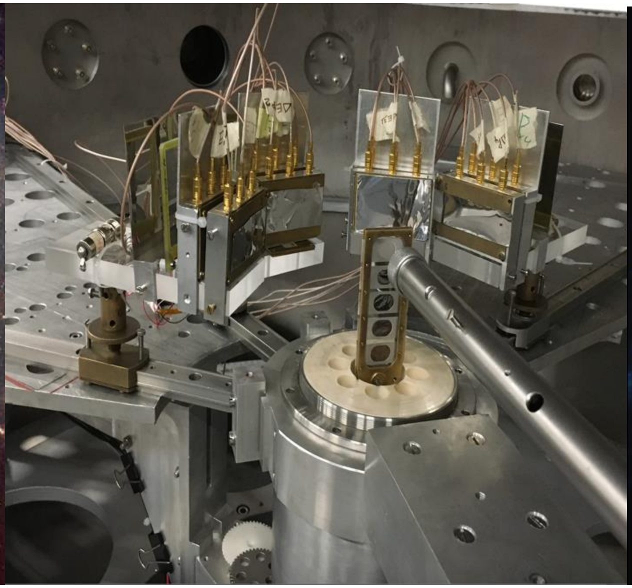

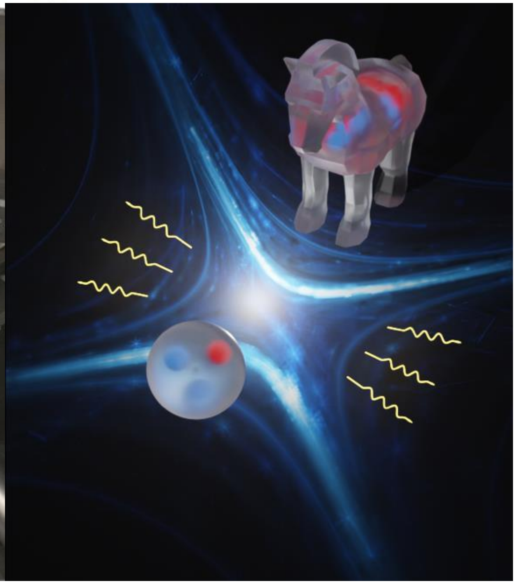

Aurora Tumino

UNIVERSITAS STUDIORUM HENNAE — LIBERA UNIVERSITÀ KORE ENNA

INFN Istituto Nazionale di Fisica Nucleare

ChETEC INFRA

Outline

- Why we need indirect techniques in Nuclear Astrophysics
- Trojan Horse Method (THM)
- C burning and other stories

The Coulomb Barrier Challenge in Nuclear Astrophysics

σ ~picobarn $\Rightarrow$ Low signal-to-noise ratio due to the Coulomb barrier between the interacting nuclei

measure $\sigma(E)$ over as wide a range as possible, then extrapolate down to E_0!

CROSS SECTION

$$\sigma(E) = \frac{1}{E} \exp(-2\pi\eta)\, S(E)$$

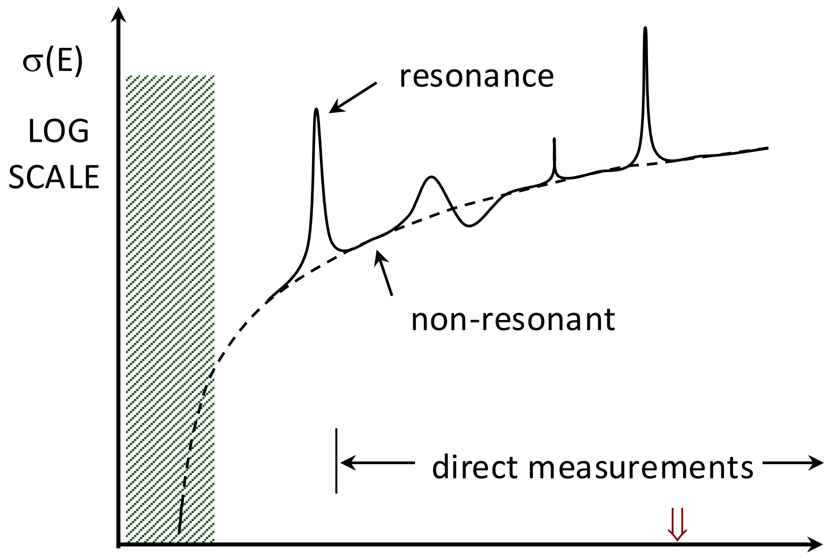

S-FACTOR

$$S(E) = E\sigma(E) \exp(2\pi\eta)$$

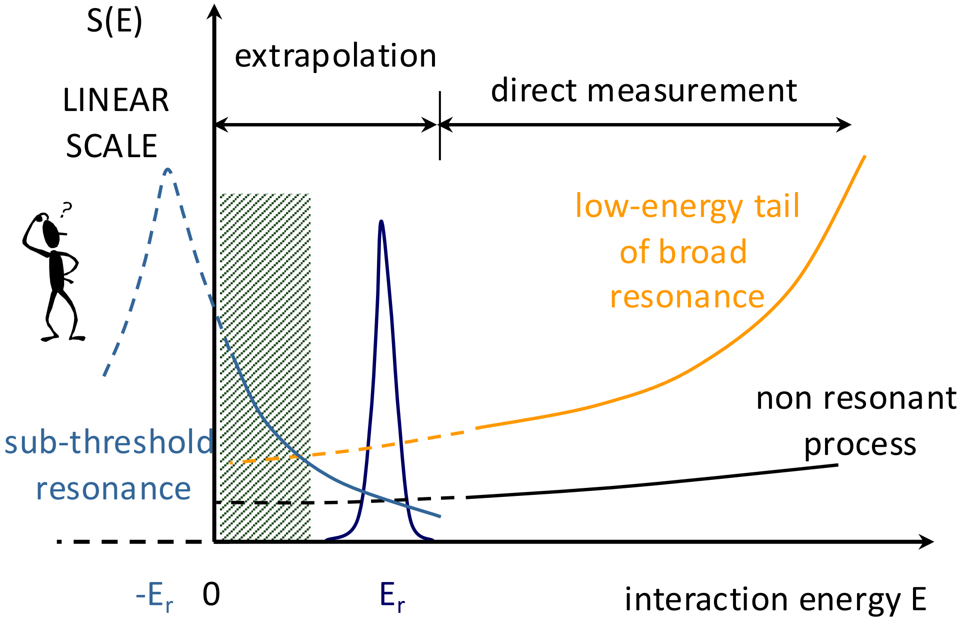

DANGER OF EXTRAPOLATION !

Barnes et al. PLB 197, 315 (1987)]

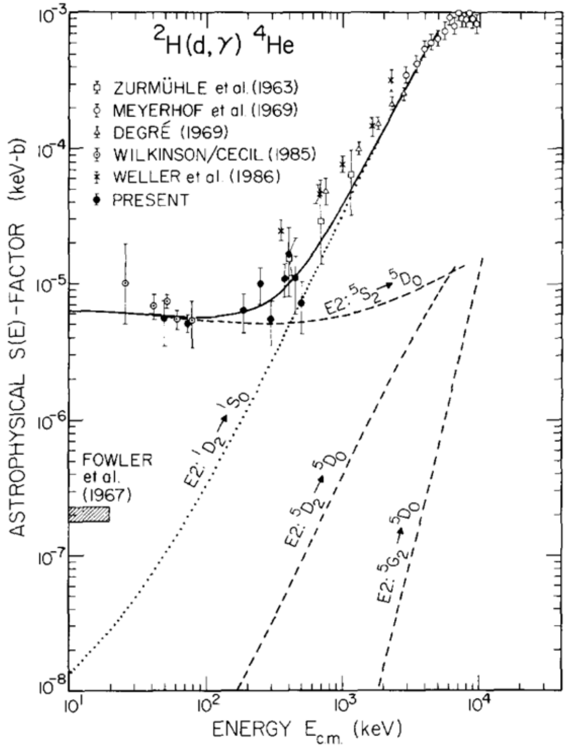

Fig. 1. Excitation function for $^2H(d,\gamma)^4He$ from the present and previous work [3–8]. The data from 1–4 MeV are described well by an E2 direct capture process, $^1D_2 \rightarrow {}^1S_0$ (dotted curve). The high cross sections at low energies are attributed to E2 radiation from an initial S-state of relative motion of the deuterons. The calculated $^5D_2 \rightarrow {}^5D_0$ and $^5G_2 \rightarrow {}^5D_0$ yields are negligible. Also shown is the previously recommended astrophysical $S(0)$ value, 2×10^{-7} keV b [9].

Electron screening: first evidence

LUNA – Phase I: 50 kV accelerator (1992-2001)

to investigate reactions in solar pp chain

R. Bonetti et al.: Phys. Rev. Lett. 82 (1999) 5205

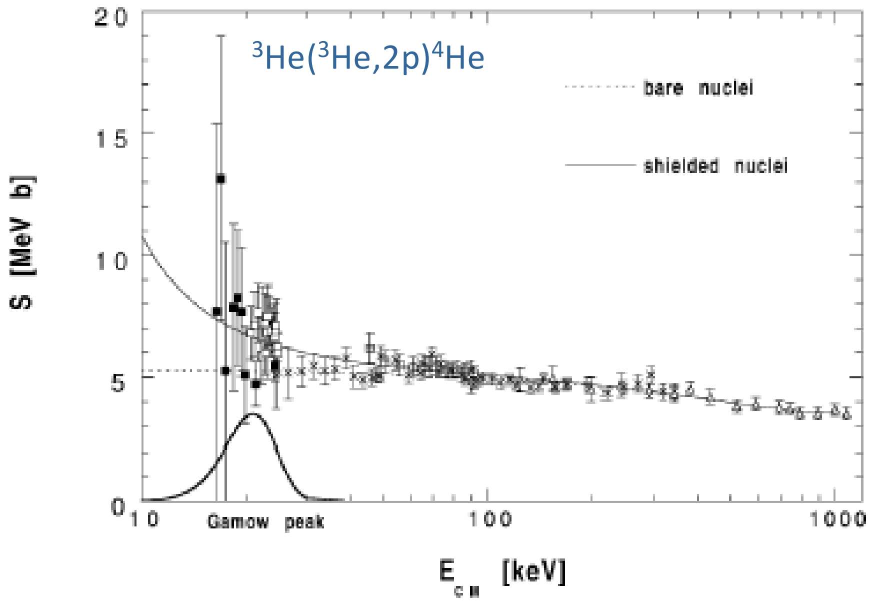

@ lowest energy:

σ ~ 20 fb → 1 count/month

No evidence for a narrow resonance suggested to explain the 8B and 7Be solar neutrino flux reduction.

First evidence of electron screening

only two reactions studied directly at the Gamow peak

… intrinsic limitation at astrophysical energies → → → → Electron Screening

S(E) experimental enhancement due to the electron screening

$$S(E)_s = S(E)_b \exp(\pi\eta U_e/E)$$

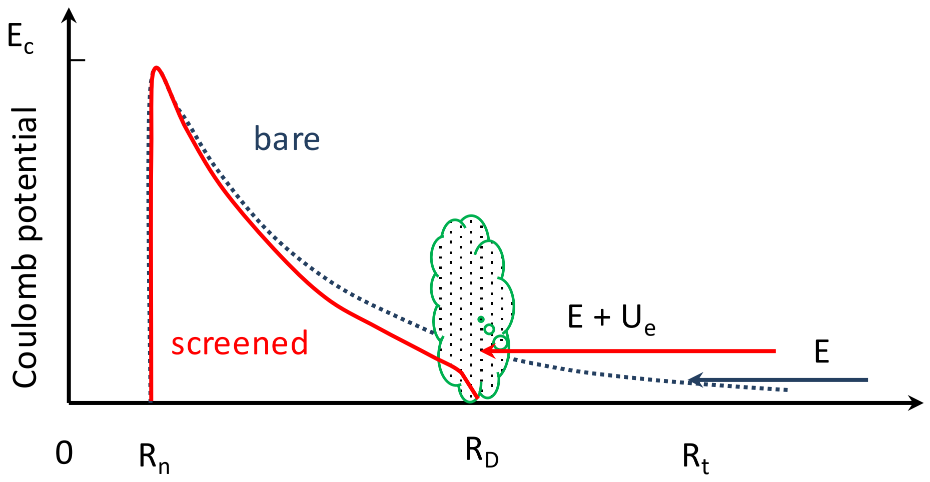

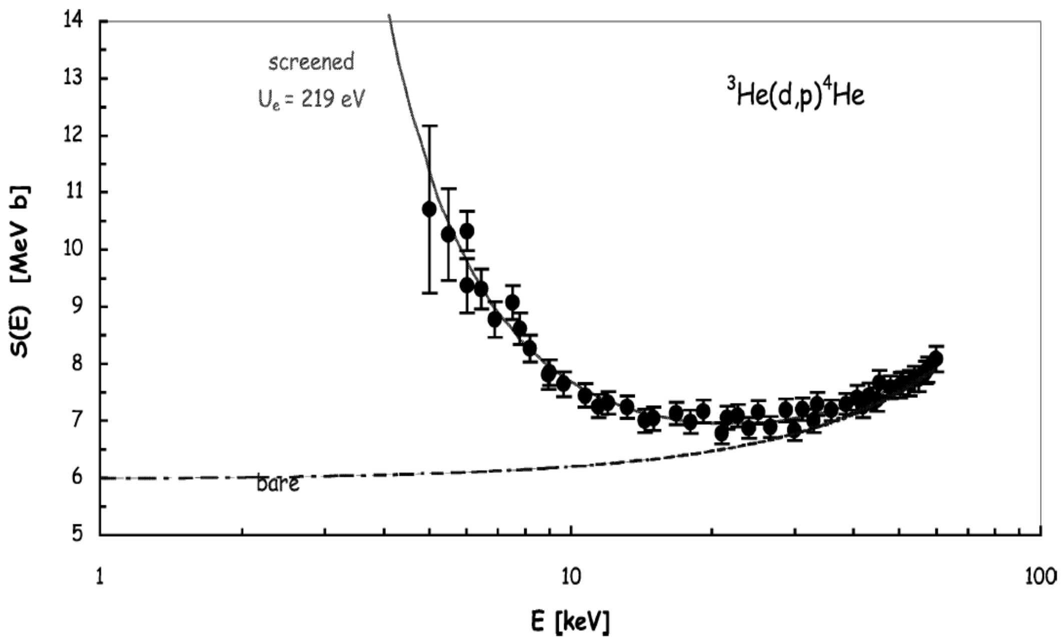

In astrophysical plasma:

- the screening, due to free electrons in plasma, can be different
→ we need $S(E)_b$ to evaluate reaction rates

→ No way to measure $S(E)_b$ from direct experiments at energies where screening is important

$S_b(E)$-factor extracted from extrapolation of higher energy data

Further Challenges to Direct Measurements

-Medium- to heavy-ion reactions: the ground-state exit channels are hard to measure directly

-A direct measurement usually uses particle-γ coincidence to control the huge background

-Reactions with radioactive ions and neutrons: no neutron targets exist for direct (n,x) measurements

-Targets from short-lived radioactive species are often unfeasible to prepare

-THM overcomes both: transferring a neutron off a deuteron gives an effective neutron beam, with no radioactive sample to handle

Indirect methods extend measurements to reactions direct techniques cannot reach

See also: A. Tumino et al., Ann. Rev. Nucl. Part. Sci. 71 (2021) 346

Indirect Methods in Nuclear Astrophysics

- No Coulomb suppression: measurements can reach down to zero relative energy without exponential decay in yield
- No electron screening: directly provides the bare-nucleus S(E) factor required for stellar models & independent information on U_e
- Overcoming possible difficulties in producing the beam or the target (radioactive ions, neutrons..)

Quite straightforward experiment, but …

Entrance channel

A+a

Several reaction mechanisms link the two channels

Reaction products

C+c+…

The reaction theory is needed to select only one reaction mechanism. However, nowadays powerful techniques and observables for careful data analysis and theoretical investigation.

THM

Basic principle: relevant low-energy two-body σ from quasi-free contribution of an appropriate three-body reaction in quasi free kinematics

$$A + a \rightarrow b + B + s \quad \rightarrow\rightarrow\rightarrow \quad A + x \rightarrow b + B$$

a: $x \oplus s$ clusters

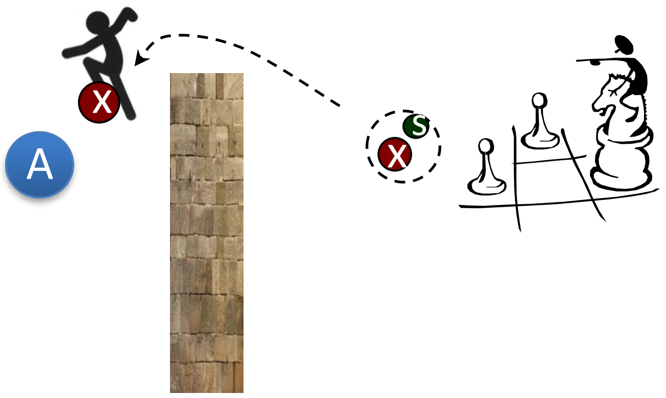

Repulsion wall

Quasi free mechanism

✓ only x - A interaction

✓ s = spectator (p_s~0)

$E_A > E_{Coul} \Rightarrow$

NO Coulomb suppression

NO electron screening

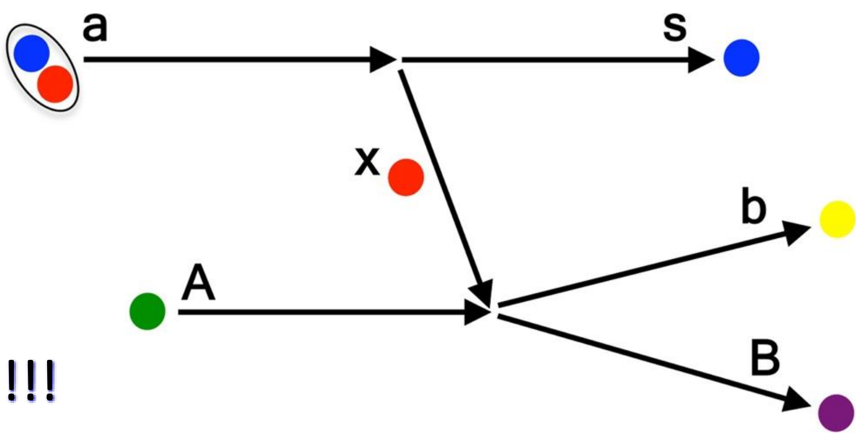

$E_{q.f.} = E_{Ax} - B_{x\text{-}s} \pm$ (intercluster motion)

plays a key role in compensating for the beam energy

$E_{q.f.} \approx 0$!!!

See for review:

R. Tribble et al., Rep. Prog. Phys. **77** (2014) 106901

A. Tumino et al. Ann. Rev. Nucl. Part. Sci. 71 (2021) 346

Theoretical approaches to the THM

$$A + a \to c + C + s \rightarrow \rightarrow \rightarrow \quad A + x \to c + C$$

PWIA hypotheses:

- beam energy > a = x $\oplus$ s breakup Q-value
- projectile wavelength k^{-1} << x – s intercluster distance

$$\frac{d^3\sigma}{d\Omega_B d\Omega_b dE_B} \propto \underbrace{KF}_{\text{kinematical factor}} \underbrace{\left|\Phi(p_{xs})\right|^2}_{\text{momentum distribution of } s \text{ inside } a} \underbrace{\left[\frac{d^2\sigma_{xA\to bB}}{dE_{xA}d\Omega}\right]^{HOES}}_{\text{Nuclear cross section for the A+x}\to\text{C+c reaction}}$$

kinematical factor

momentum distribution of *s* inside *a*

Nuclear cross section for the A+x→C+c reaction

MPWBA formalism

(S. Typel and H. Wolter, Few-Body Syst. 29 (2000) 75)

- distortions introduced in the c+C channel, but plane waves for the three-body entrance/exit channel

- off-energy-shell effects corresponding to the suppression of the Coulomb barrier are included

A. Tumino et al., PRL 98, 252502 (2007)

but <u>No absolute value of the cross section</u>

Theoretical approaches to the THM

R. Tribble et al., Rep. Prog. Phys. **77** (2014) 106901

The THM simple factorization can be deduced from the general formula in the case of resonant reactions

Amplitude of the TH reaction

$$M^{\mathrm{PWA(prior)}}(P, \boldsymbol{k}_{aA}) = (2\pi)^2 \sqrt{\frac{1}{\mu_{bB} k_{bB}}}\, \varphi_a(\boldsymbol{p}_{sx})$$
$$\times \sum_{J_F M_F j' l l' m_{j'} m_l m_{l'} M_n} i^{l+l'} \langle j m_j l m_l | J_F M_F \rangle \langle j' m_{j'} l' m_{l'} | J_F M_F \rangle$$
$$\times \langle J_x M_x J_A M_A | j' m_{j'} \rangle \langle J_s M_s J_x M_x | J_a M_a \rangle\, \mathrm{e}^{-\mathrm{i}\delta^{hs}_{bBl}} Y_{l m_l}(-\hat{\boldsymbol{k}}_{bB})$$
$$\times \sum_{\nu,\tau=1}^{N} [\Gamma_{\nu bBjlJ_F}(E_{bB})]^{1/2} [\boldsymbol{A}^{-1}]_{\nu\tau} Y^{*}_{l' m_{l'}}(\hat{\boldsymbol{p}}_{xA})$$
$$\times \sqrt{\frac{R_{xA}}{\mu_{xA}}} [\Gamma_{\nu xAl'j'J_F}(E_{xA})]^{1/2} P_{l'}^{-1/2}(k_{xA}, R_{xA}) (j_{l'}(p_{xA} R_{xA})$$
$$\times [(B_{xAl'}(k_{xA}, R_{xA}) - 1) - D_{xAl'}(p_{xA}, R_{xA})]$$
$$+ 2 Z_x Z_A e^2 \mu_{xA} \int_{R_{xA}}^{\infty} \mathrm{d}r_{xA} \frac{O_{l'}(k_{xA}, r_{xA})}{O_{l'}(k_{xA}, R_{xA})} j_{l'}(p_{xA} r_{xA})).$$

This accounts for:

- HOES effects
- Normalization (very useful for RIBS)

Moreover:
Possible generalization to CDCC & DWBA

However → More complicated!

… for Resonant Reactions

The A + a(x+s) $\rightarrow$ F*(c + C) + s process is a transfer to the continuum where particle x is the transferred particle

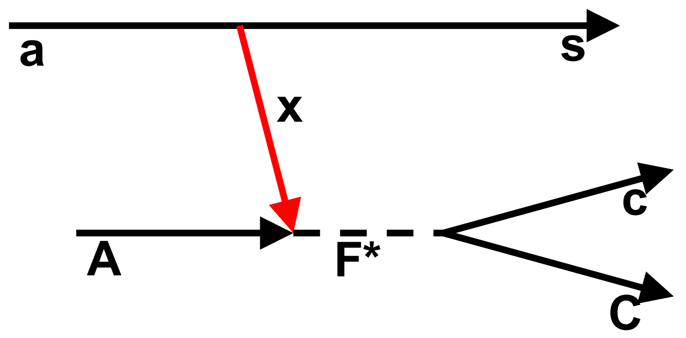

Standard R-Matrix approach cannot be applied to extract the resonance parameters → Modified R-Matrix is introduced instead

In the case of a resonant THM reaction the cross section takes the form

$$\frac{d^2\sigma}{dE_{Cc}\,d\Omega_s} \propto \frac{\Gamma_{(Cc)_i}(E)\,|M_i(E)|^2}{(E-E_{R_i})^2+\Gamma_i^2(E)/4}$$

$M_i(E)$ is the amplitude of the transfer reaction (upper vertex) that can be easily calculated
→ The resonance parameters can be extracted

When transfer to a bound F state, M^2 is proportional to the ANC of the populated F state

Advantages:
- possibility to measure down to zero energy
- No electron screening
- HOES reduced widths are the same entering the OES S(E) factor (New!)

Reactions studied with the THM.

	Indirect reaction	Direct reaction	References
[1]	$^{2}H(^{7}Li,\alpha\alpha)n$	$^{1}H(^{7}Li,\alpha)^{4}He$	Spitaleri et al 1999, Lattuada et al 2001 [97]
[2]	$^{3}He(^{7}Li,\alpha\alpha)d$	$^{2}H(^{7}Li,\alpha)^{4}He$	Tumino et al 2006 [98]
[3]	$^{2}H(^{6}Li,\alpha^{3}He)n$	$^{1}H(^{6}Li,\alpha)^{3}He$	Tumino et al 2003 [88]
[4]	$^{6}Li(^{6}Li,\alpha\alpha)^{4}He$	$^{2}H(^{6}Li,\alpha)^{4}He$	Spitaleri et al 2001 [22]
[5]	$^{2}H(^{9}Be,\alpha^{6}Li)n$	$^{1}H(^{9}Be,\alpha)^{6}Li$	Wen et al 2008 [99]
[6]	$^{2}H(^{10}B,\alpha^{7}Be)n$	$^{1}H(^{10}B,\alpha)^{7}Be$	Lamia et al 2008, Rapisarda et al 2018, Cvetinovic et al 2018 [100–102]
[7]	$^{2}H(^{11}B,\alpha_{0}{}^{8}Be)n$	$^{1}H(^{11}B,\alpha)^{8}Be$	Spitaleri et al 2004, Lamia et al 2011 [103,104]
[8]	$^{2}H(^{15}N,\alpha^{12}C)n$	$^{1}H(^{15}N,\alpha)^{12}C$	La Cognata et al 2007 [105]
[9]	$^{2}H(^{18}O,\alpha^{15}N)n$	$^{1}H(^{18}O,\alpha)^{15}N$	La Cognata et al 2009 [106]
[10]	$^{2}H(^{17}O,\alpha^{14}N)n$	$^{1}H(^{17}O,\alpha)^{14}N$	Sergi et al 2010, Sergi et al. 2015 [89,90]
[11]	$^{6}Li(^{3}He,p^{4}He)^{4}He$	$^{2}H(^{3}He,p)^{4}He$	La Cognata et al 2005 [107]
[12]	$^{2}H(^{6}Li,p^{3}H)^{4}He$	$^{2}H(d,p)^{3}H$	Rinollo et al 2005 [108]
[13]	$^{6}Li(^{12}C,\alpha^{12}C)^{2}H$	$^{4}He(^{12}C,{}^{12}C)^{4}He$	Spitaleri et al 2000 [109]
[14]	$^{2}H(^{6}Li,t^{4}He)^{1}H$	$n(^{6}Li,t)^{4}He$	Tumino et al 2005, Gulino et al 2010 [110,111]
[15]	$^{2}H(p,pp)n$	$^{1}H(p,p)^{1}H$	Tumino et al 2007, Tumino et al 2008 [112,113]
[16]	$^{2}H(^{3}He,p^{3}H)^{1}H$	$^{2}H(^{2}H,p)^{3}H$	Tumino et al 2011, Tumino et al 2014 [94,114]
[17]	$^{2}H(^{3}He,n^{3}He)^{1}H$	$^{2}H(^{2}H,n)^{3}He$	Tumino et al 2011, Tumino et al 2014 [94,114]
[18]	$^{2}H(^{19}F,\alpha^{16}O)n$	$^{1}H(^{19}F,\alpha)^{16}O$	La Cognata et al 2011, Indelicato et al 2017 [32,115]
[19]	$^{13}C(^{6}Li,n^{16}O)^{2}H$	$^{13}C(\alpha,n)^{16}O$	La Cognata et al 2014 [116]
[20]	$^{2}H(^{18}F,\alpha^{15}O)n$	$^{1}H(^{18}F,\alpha)^{15}O$	Cherubini et al 2015, Pizzone et al. 2016, La Cognata et al. 2017 [92,117,118]
[21]	$^{2}H(^{10}B,\alpha^{7}Li)^{1}H$	$n(^{10}B,\alpha)^{7}Li$	Guardo et al 2019, Sparta et al 2021 [119,120]
[22]	$^{2}H(^{7}Be,\alpha\alpha)^{1}H$	$n(^{7}Be,\alpha)^{4}He$	Lamia et al 2017, Lamia et al 2019, Hayakawa et al 2021 [121–123]
[23]	$^{12}C(^{14}N,\alpha^{20}Ne)^{2}H$	$^{12}C(^{12}C,\alpha)^{20}Ne$	Tumino et al 2018 [30]
[24]	$^{12}C(^{14}N,p^{23}Na)^{2}H$	$^{12}C(^{12}C,p)^{23}Na$	Tumino et al 2018 [30]
[25]	$^{6}Li(^{19}F,p^{22}Ne)^{2}H$	$^{4}He(^{19}F,p)^{22}Ne$	Pizzone et al 2017, Dagata et al 2018 [117,124]
[26]	$^{2}H(^{17}O,\alpha^{14}C)^{1}H$	$^{17}O(n,\alpha)^{14}C$	Oliva et al 2020 [125]
[27]	$^{2}H(^{3}He,pt)^{1}H$	$^{3}He(n,p)^{3}H$	Pizzone et al 2021 [126]
[28]	$^{2}H(^{7}Be,p^{7}Li)^{1}H$	$n(^{7}Be,p)^{7}Li$	Hayakawa et al 2021 [123]
[29]	$^{2}H(^{27}Al,\alpha^{24}Mg)n$	$^{27}Al(p,\alpha)^{24}Mg$	Palmerini et al 2021, La Cognata et al. 2022 [127–129]

12C+12C fusion

C-burning crucial phase in the nucleosynthesis of massive stars (> 8 $M_{\odot}$), determines M_{up}, ignition trigger for superbursts and Type Ia supernovae

astrophysical energy: 1 – 3 MeV

From direct measurement, minimum E: 2.1 MeV

extrapolations differ by 3 orders of magnitude

without inclusion of resonances

Indirect measurement with THM down to 1 MeV:

$^{12}C(^{14}N,\alpha\,^{20}Ne)^{2}H$ and $^{12}C(^{14}N,p\,^{23}Na)^{2}H$.

Resonances dominate the astrophysical energy

$^{12}C + ^{12}C \rightarrow \alpha + ^{20}Ne$

$^{12}C + ^{12}C \rightarrow p + ^{23}Na$

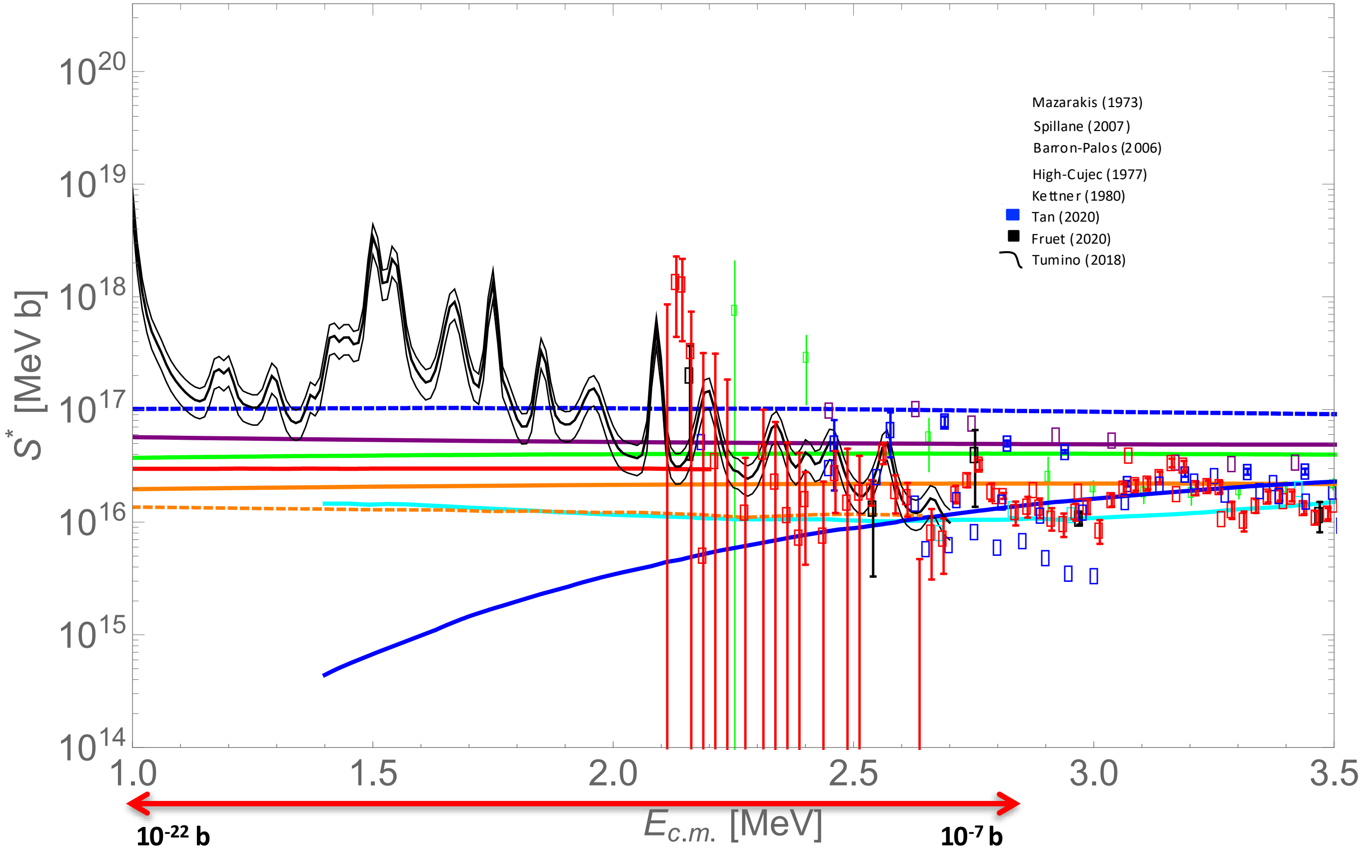

nature

International journal of science

Letter | Published: 23 May 2018

An increase in the $^{12}C + ^{12}C$ fusion rate from resonances at astrophysical energies

A. Tumino, C. Spitaleri, M. La Cognata, S. Cherubini, G. L. Guardo, M. Gulino, S. Hayakawa, I. Indelicato, L. Lamia, H. Petrascu, R. G. Pizzone, S. M. R. Puglia, G. G. Rapisarda, S. Romano, M. L. Sergi, R. Spartá & L. Trache

Nature **557**, 687–690 (2018) | Download Citation

12C+12C comprehensive figure

$^{12}C + ^{12}C \rightarrow \alpha + ^{20}Ne$

$^{12}C + ^{12}C \rightarrow p + ^{23}Na$

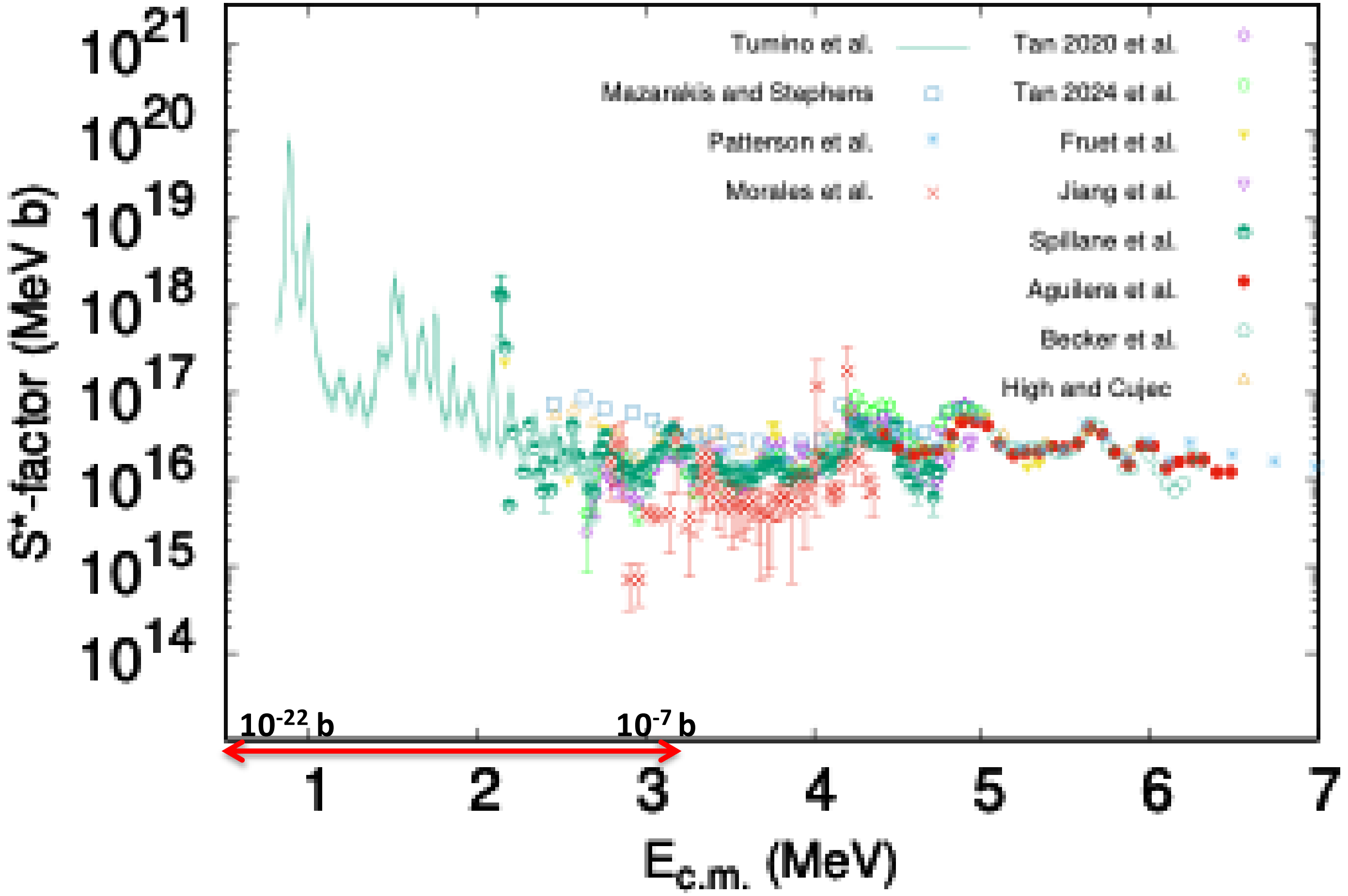

Our Experiment with theTHM

$^{12}C(^{12}C,\alpha)^{20}Ne$ and **$^{12}C(^{12}C,p)^{23}Na$** reactions via the Trojan Horse Method applied to the **$^{12}C(^{14}N,\alpha^{20}Ne)^{2}H$** and **$^{12}C(^{14}N,p^{23}Na)^{2}H$** three-body processes

^{2}H from the ^{14}N as spectator s

Observation of ^{12}C cluster transfer in the $^{12}C(^{14}N,d)^{24}Mg^{*}$ reaction (R.H. Zurmûhle et al. PRC 49 (1994) 5)

E_{14N} =30 MeV> E_{coul} d,p/α coincidence detection

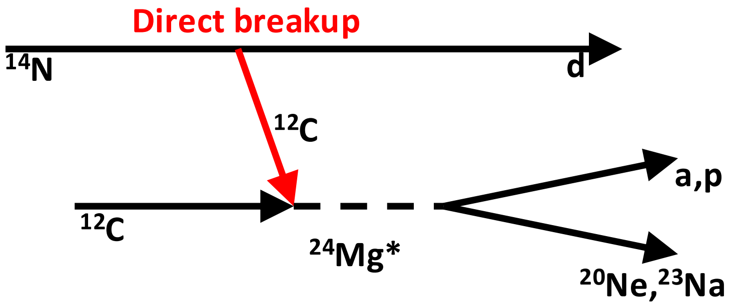

$$E_{QF} = E_{14N}\frac{m_{^{12}C}}{m_{^{14}N}} \cdot \frac{m_{^{12}C}}{m_{^{12}C}+m_{^{12}C}} - 10.27\ \text{MeV}$$

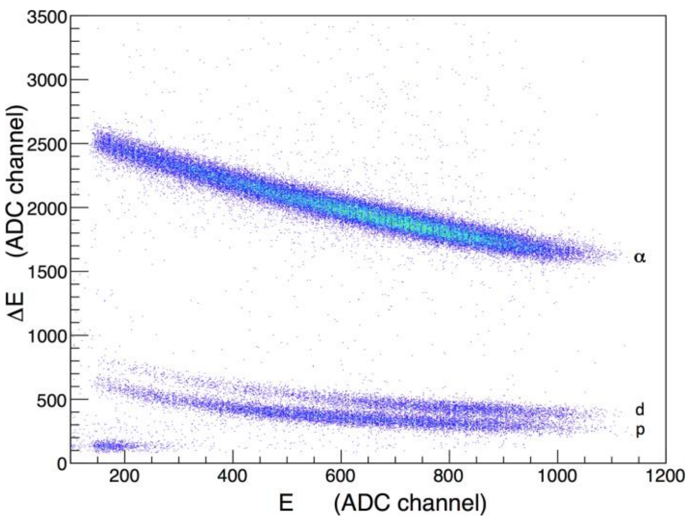

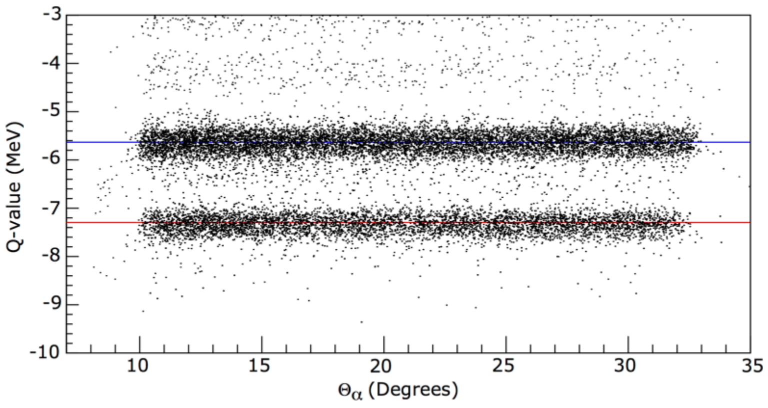

A. Tumino et al., Nature (2018)

Selection of the quasi-free mechanism

Comparison between the experimental momentum distribution and the theoretical one

$$|\Phi(\overrightarrow{p_d})|^2 \propto \frac{\dfrac{d^3\sigma}{d\Omega_d d\Omega_{p,\alpha} dE_d}}{(KF)\left(\dfrac{d\sigma_{12C12C}}{d\Omega}\right)^N}$$

On-the-energy-shell bound state wave number ((see I.S. Shapiro, Soviet Physics Uspekhi Vol. 10, n. 4 (1968) and earlier works): $(2\mu_{d12C}B_{d12C})^{1/2}$=181 MeV/c.
Staying within this value is the condition for the QF mechanism to be dominant

Solid line: momentum distribution of d inside ^{14}N from the Wood-Saxon ^{12}C-d bound state potential with standard geometrical parameters r_0=1.25 fm, a=0.65 fm and V_0=54.427 MeV

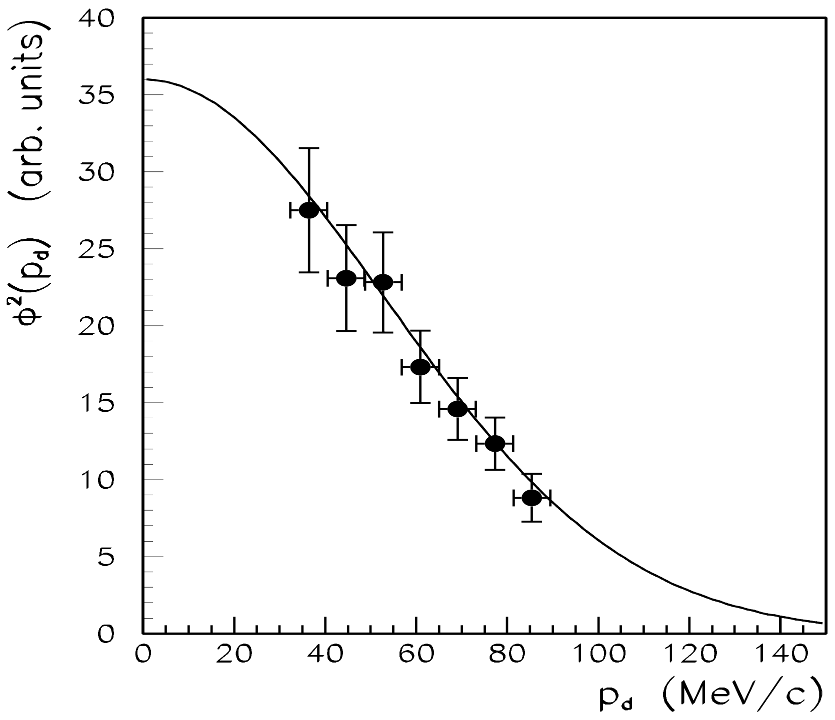

Plane Waves reliable also because:

- $p_d < (2\mu_{d12C}B_{d12C})^{1/2}$=181 MeV/c → Proved that the shape of the momentum distribution is insensitive to the theoretical framework used for its derivation (agreement between PWA and DWBA)

- the ^{14}N beam energy of 30 MeV corresponds to a quite high momentum transfer q_t=500 MeV/c giving an associate de Broglie wavelenght of 0.4 fm (< 3 fm=^{12}C+d)

Recent theoretical developements to investigate the $^{12}C+^{12}C$ fusion:

Debate around THM results:

theory calculations based on DWBA (Mukhamedzhanov et al., PRC 2019): large corrections (red squares) to the initially reported S-factors. However, several points are obscure, such as:

-the numerical stability of the calculations involving a transfer to the continuum is not guaranteed and needs a more critical examination.
-12C+12C unusual potential parameters: extremely large diffuseness and radius;
-bin functions to reproduce resonances with an unphysically large number of nodes, thus highly oscillatory pattern responsible for the huge decrease of the transfer process.

(Bonasera and Natowitz PRC(R) 2020)

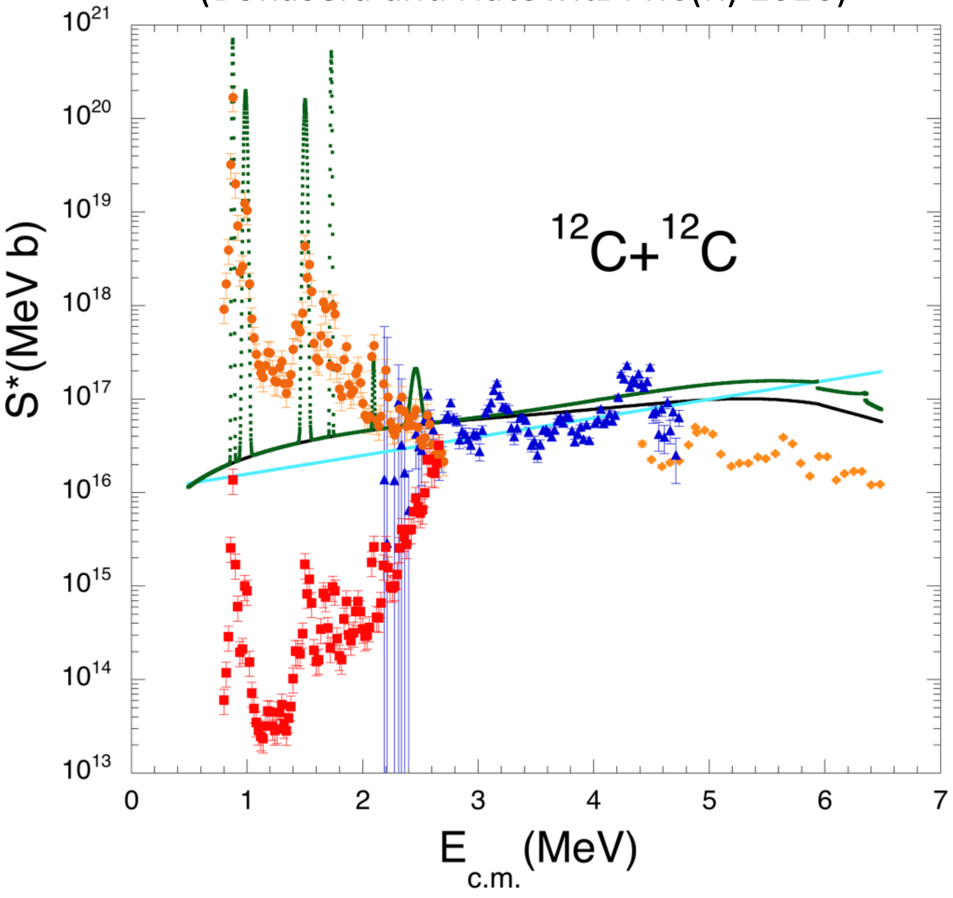

Theory calculations using the Feynman path-integral method (Bonasera and Natowitz PRC(R) 2020) and including some l=0 resonances, lead to S-factor values (green color) in agreement with results from the THM experiment (orange circles), highlighting the role of resonances

The drop can be due to the assumption of having an isolated resonance or to an incomplete inclusion of Coulomb effects (only those from intermediate channel are in)

With a full account of intermediate and final state Coulomb effects, the drop disappears →→

A way to account for Coulomb effects in a whole

Few-Body Syst (2019) 60:27
https://doi.org/10.1007/s00601-019-1489-9

Check for updates

A. M. Mukhamedzhanov · A. S. Kadyrov

Theory of Surrogate Nuclear and Atomic Reactions with Three Charged Particles in the Final State Proceeding Through a Resonance in the Intermediate Subsystem

This work provides formulas to evaluate the impact of the Coulomb interaction in an analytic form for a THM reaction:

$$a + A \to s + F^* \to s + b + B$$

4. The triply differential cross section for the TH reaction is given by

$$\frac{d^3\sigma}{d\Omega_{\mathbf{k}_{sF(f)}} d\Omega_{\mathbf{k}_{bB(f)}} dE_{sF(f)}} = \sigma_0 \frac{\Gamma_{bB}}{[E_{0(bB)} - E_{bB(f)}]^2 + \Gamma^2/4} \frac{\pi\zeta}{\text{sh}\zeta} e^{2\zeta \arctan\frac{2\mathscr{E}}{\Gamma}}, \tag{76}$$

Where:

$$\mathscr{E} = E_{0(bB)} - E_{bB(f)}$$

$$\zeta = \eta_{bs} + \eta_{Bs} - \eta_{\text{R}}$$ → combination of Sommerfeld parameters

$$\eta_{\text{R}} = (Z_s Z_F/137)\,\mu_{sF}/k_{\text{R}}$$

states. If η_{bs}, η_{Bs} and $\text{Re}(\eta_{\text{R}})$ have the same sign, the Coulomb $s - F^*$ interaction in the intermediate state weakens the impact of the final state Coulomb $s - b$ and $s - B$ interactions because the intermediate state Coulomb parameter η_{R} is subtracted from the final-state Coulomb parameters $\eta_{bs} + \eta_{Bs}$, see Eq.

Moreover: if one of the Coulomb parameters in the final state, for example η_{bs}, is zero or very small then the cumulative effect of the Coulomb interactions in the intermediate and final states is negligible.

If we calculate the parameter ζ from our data: we are in the condition to have negligible Coulomb cumulative effect

p_0 channel

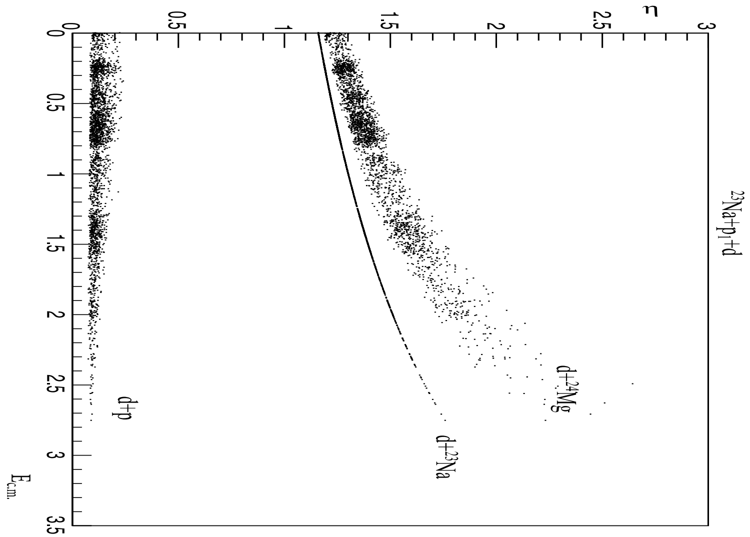

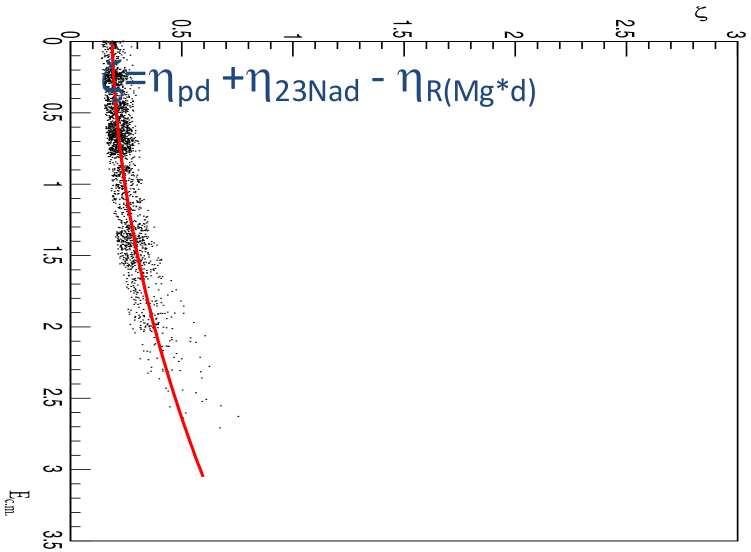

As easily inferred from the previous slide, the impact is minimal → only tails of the resonances are affected within statistical errors

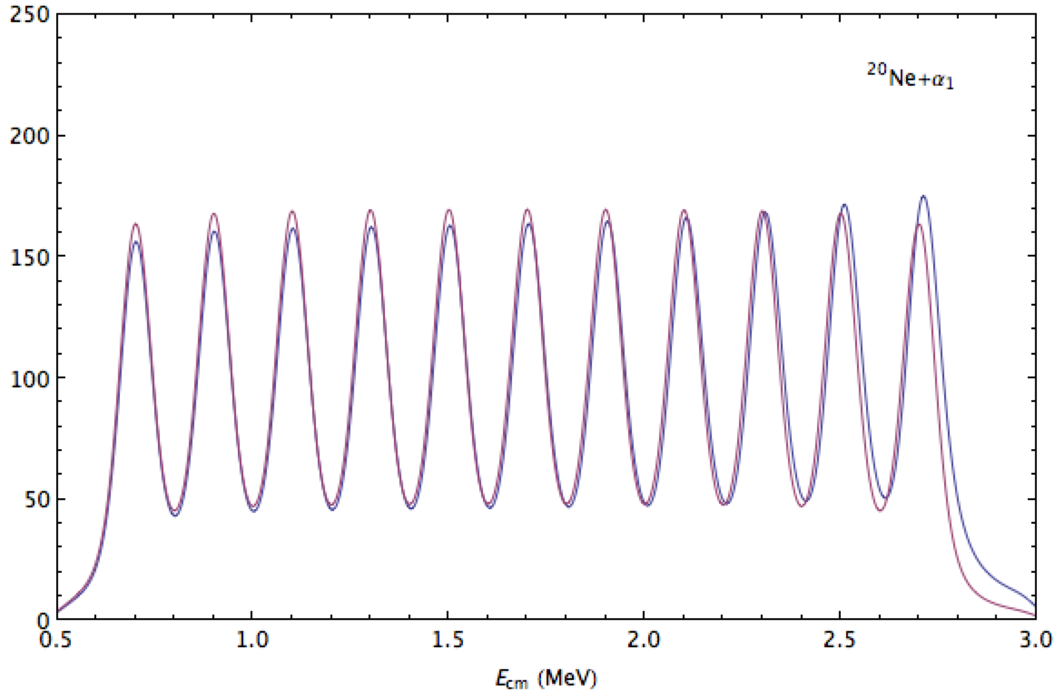

Red line: no Coulomb
Blue line: with Coulomb
No change within experimental errors

The Coulomb distortion only in the tails

The Coulomb contribution affecting only the tails of the resonances …

This is what is reported in K. Hagino PRC112, 034611 (2025).

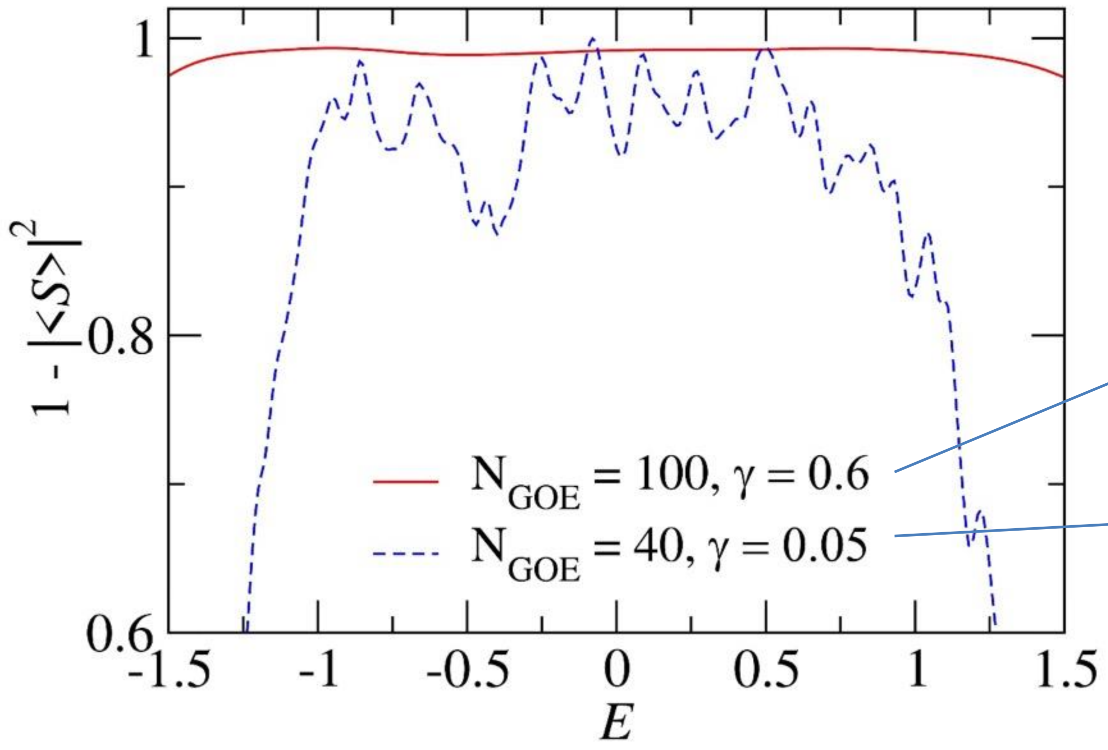

The transmission factor is approaching one at the resonance tips!

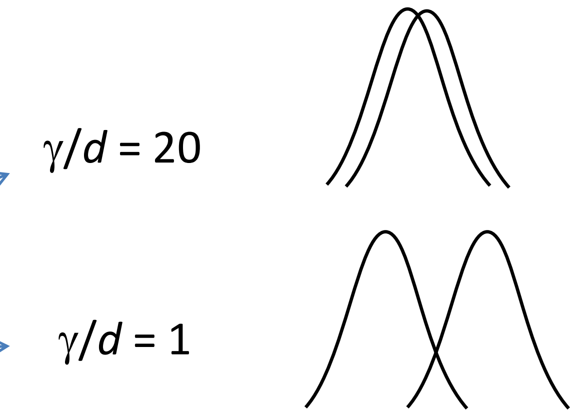

nature
International journal of science

Letter | Published: 23 May 2018

An increase in the $^{12}C + {}^{12}C$ fusion rate from resonances at astrophysical energies

A. Tumino, C. Spitaleri, M. La Cognata, S. Cherubini, G. L. Guardo, M. Gulino, S. Hayakawa, I. Indelicato, L. Lamia, H. Petrascu, R. G. Pizzone, S. M. R. Puglia, G. G. Rapisarda, S. Romano, M. L. Sergi, R. Spartá & L. Trache

Nature **557**, 687–690 (2018) | Download Citation

12C+12C Reaction Rate

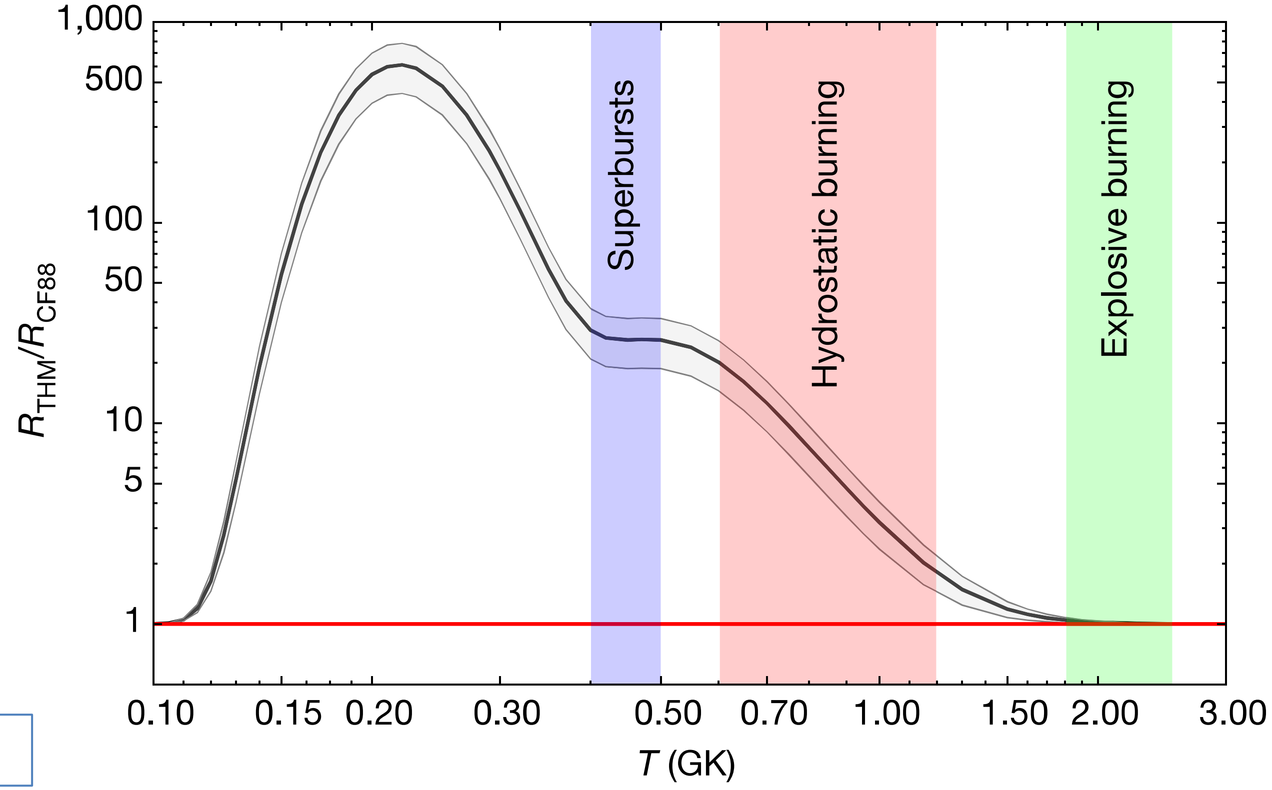

Color shadings mark typical regions for C-burning

Compared to CF88, the present rate increases from a factor of 1.18 at 1.2 GK to a factor of more than 25 at 0.5 GK

Some implications from the new 12C+12C rate

- Solution of the Neutron star birthrate problem (K. Mori et al. MNRAS 2018)?:

The NS birthrate has been estimated to be $10.8^{+7.0}_{-5.0}$ NSs/century, while the CCSN rate is estimated to be 1.9±1.1 SNe/century from measurements of γ-ray from ^{26}Al (Diehl et al. 2006; Keane & Kramer 2008), suggesting that the origin of NSs is supplemented by the so called Accretion Induced Collapse path of the WD mergers.

The enhanced reaction rate results in a lower ignition temperature, leading to a higher probability of finding WD-WD mergers reaching the Accretion Induced Collapse. This could increase the birthrate of the Galactic Neutron stars making the fraction of the WD mergers in the progenitors of type Ia SNe smaller.

-New investigation of the dependence of the compactness on the initial mass:

red dots → CF88
blue dots →THM

(A. Chieffi et al. ApJ 2021)

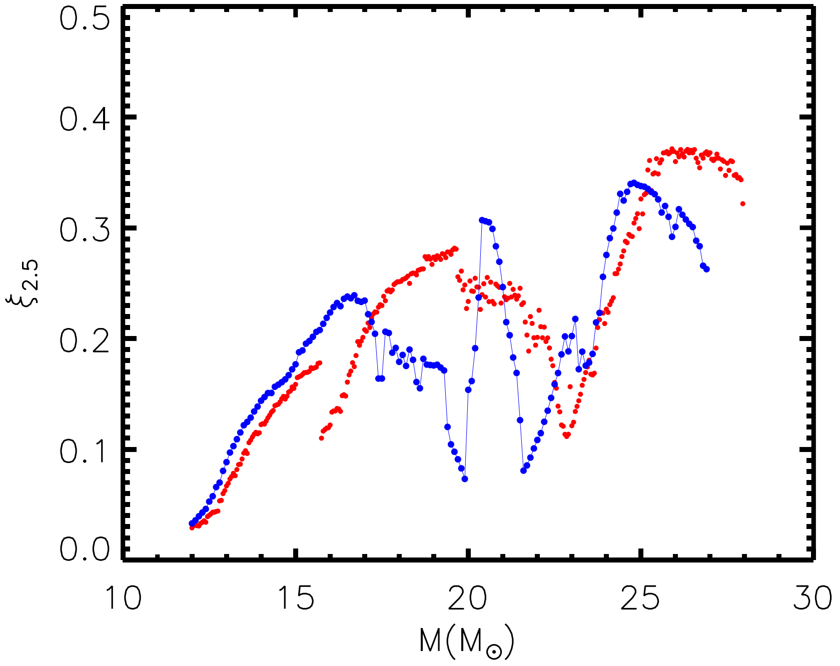

It is quite evident that the adopted nuclear cross section plays an important role in determing the final compactness of a star and hence its final fate: explosion or collapse. Remarkable lower compactness in some mass intervals, like between 17 and 20 $M_\odot$, and 21 and 23$M_\odot$, and above 25$M_\odot$

Threshold masses

(Schwarzchild criterion adopted to fix the borders of the convective regions):

	$^{12}C+^{12}C$ fusion		
	HINDRANCE	**CF88**	**THM**
M_{UP} CO-WD / ONeMg WD	**8.5/9.0 $M_\odot$**	**8.0/8.5 $M_\odot$**	**7.0/7.5 $M_\odot$**
M_{CC} Minimum core collapse star	**10.5/11.0 $M_\odot$**	**10.0/10.5 $M_\odot$**	**9.5/10.0 $M_\odot$**

A. Chieffi et al, EpJ A (2025)

Masses of SN type II P

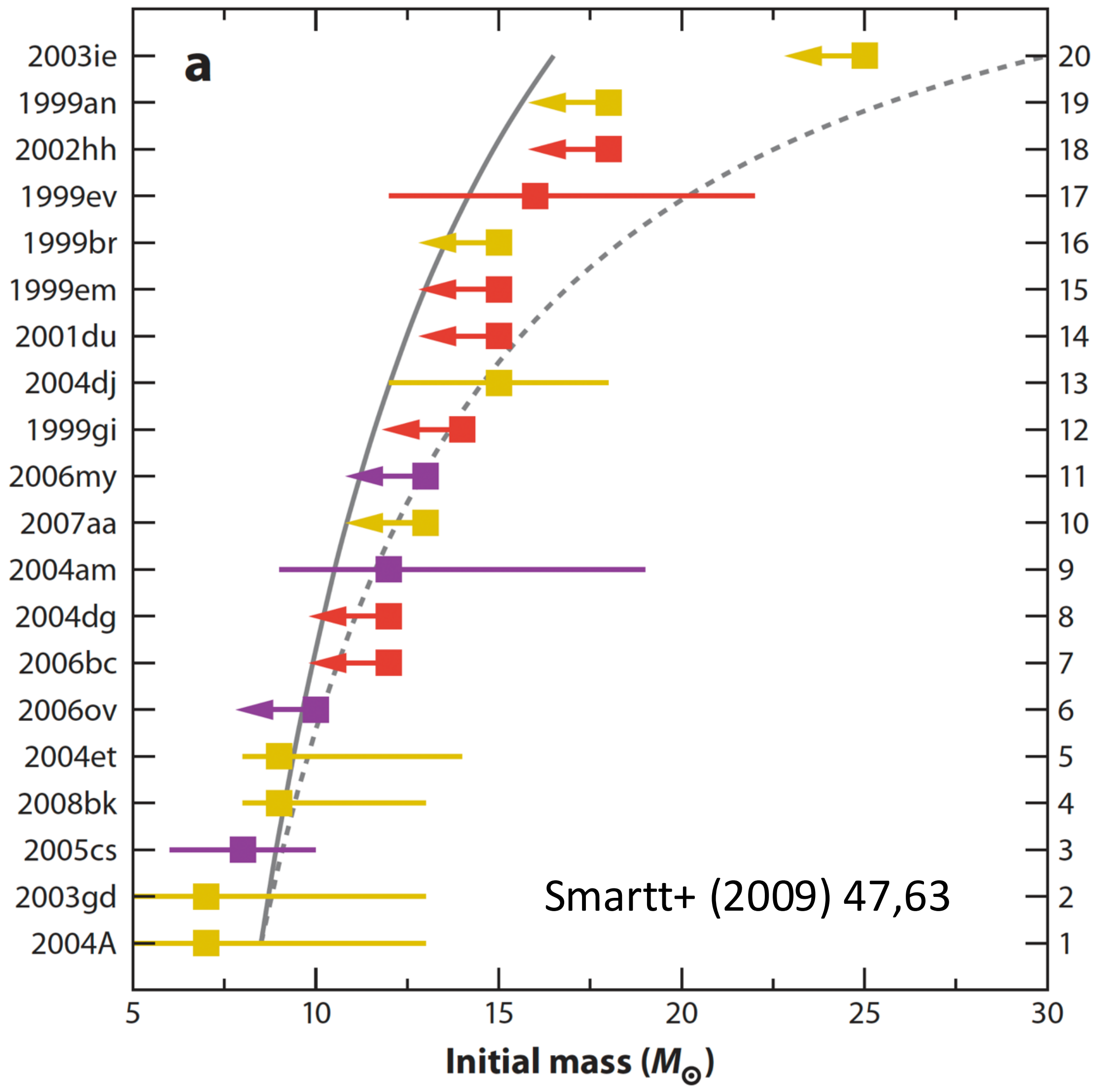

A. Chieffi courtesy

Charge independence and charge symmetry

After removing the electromagnetic interactions, the NN force between nn, np, pp are almost the same

Charge independence: equality between pp/nn force and np force

Violation: associated to the mass difference between charged and neutral pions

(identical nucleons exchange a neutral pion, a neutron and a proton may exchange both a neutral and a charged pion)

Charge symmetry: equality between pp and nn forces

Charge symmetry breaking: mainly attributed to the up-down quark mass difference

Its validity is supported to some extent by an approximate equality of binding energies of isobar nuclei.

Charge symmetry breaking manifested in the s-wave scattering lengths, a_{NN} that determine the low-energy behavior of NN scattering.

a_{np} directly determined from experiments

a_{pp} not directly accessible from experiments because of Coulomb effects → need to remove them theoretically to reveal the strong interaction contribution to the scattering length

a_{nn} not directly accessible from experiments because of the absence of neutron targets.

… we propose an innovative way to determine a_{pp} →

Two-body cross-section from THM data

THM p-p cross-section from the p+d→p+p+n quasi free reaction

Coulomb effects appear suppressed

Calculated HOES p-p cross section:

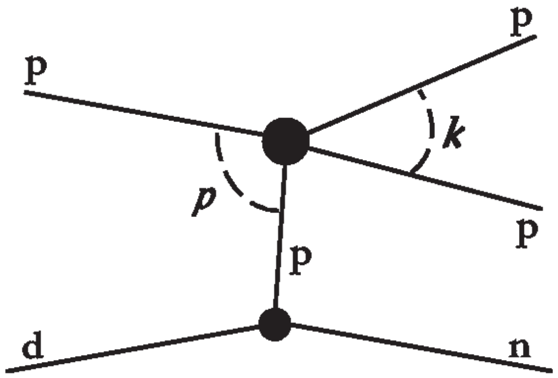

$$\left(\frac{d\sigma}{d\Omega_{\text{c.m.}}}\right)^{\text{HOES}}$$
$$= \frac{1}{k^2}\Bigg(\frac{1}{4}\Bigg[\Bigg|2\mu_{pp}\, e^2\, e^{-\pi\eta}\Gamma(1+i\eta)$$
$$\times\left(\frac{(p^2-k^2)^{i\eta}}{(\mathbf{p}-\mathbf{k})^{2(1+i\eta)}}+\frac{(p^2-k^2)^{i\eta}}{(\mathbf{p}+\mathbf{k})^{2(1+i\eta)}}\right)-2\,T_{CN}(k,\,p)\Bigg|^2\Bigg]$$
$$+\frac{3}{4}\Bigg[\Bigg|2\mu_{pp}\, e^2\, e^{-\pi\eta}\Gamma(1+i\eta)$$
$$\times\left(\frac{(p^2-k^2)^{i\eta}}{(\mathbf{p}-\mathbf{k})^{2(1+i\eta)}}-\frac{(p^2-k^2)^{i\eta}}{(\mathbf{p}+\mathbf{k})^{2(1+i\eta)}}\right)\Bigg|^2\Bigg]\Bigg). \qquad (22)$$

A. Tumino et al. PRL 98, 252502 (2007)
A. Tumino et al. PRC 78, 64001 (2008)

Red line: HOES p-p cross section
Black line: OES p-p cross section

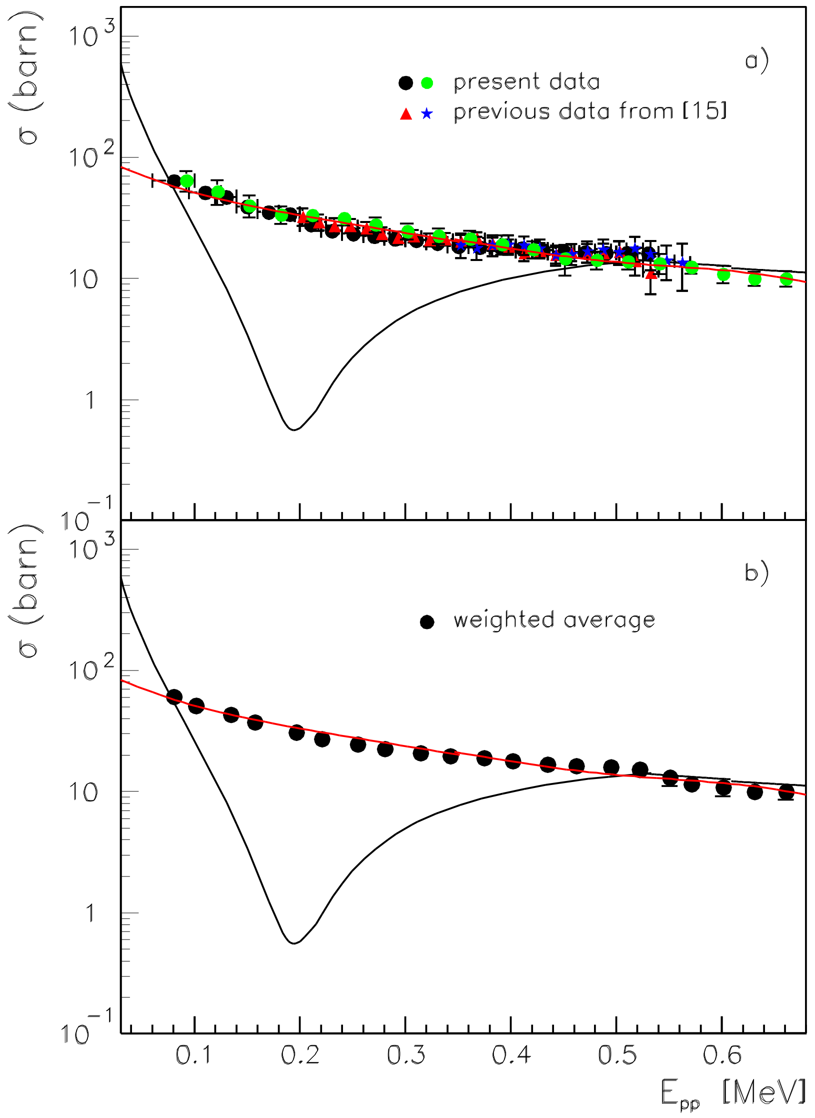

Article | Open Access | Published: 18 May 2023

Coulomb-free $^1S_0$ $p-p$ scattering length from the quasi-free $p+d \rightarrow p+p+n$ reaction and its relation to universality

Aurora Tumino, Giuseppe G. Rapisarda, Marco La Cognata, Alessandro Oliva, Alejandro Kievsky, Carlos A. Bertulani, Giuseppe D'Agata, Mario Gattobigio, Giovanni L. Guardo, Livio Lamia, Dario Lattuada, Rosario G. Pizzone, Stefano Romano, Maria L. Sergi, Roberta Spartá & Michele Viviani

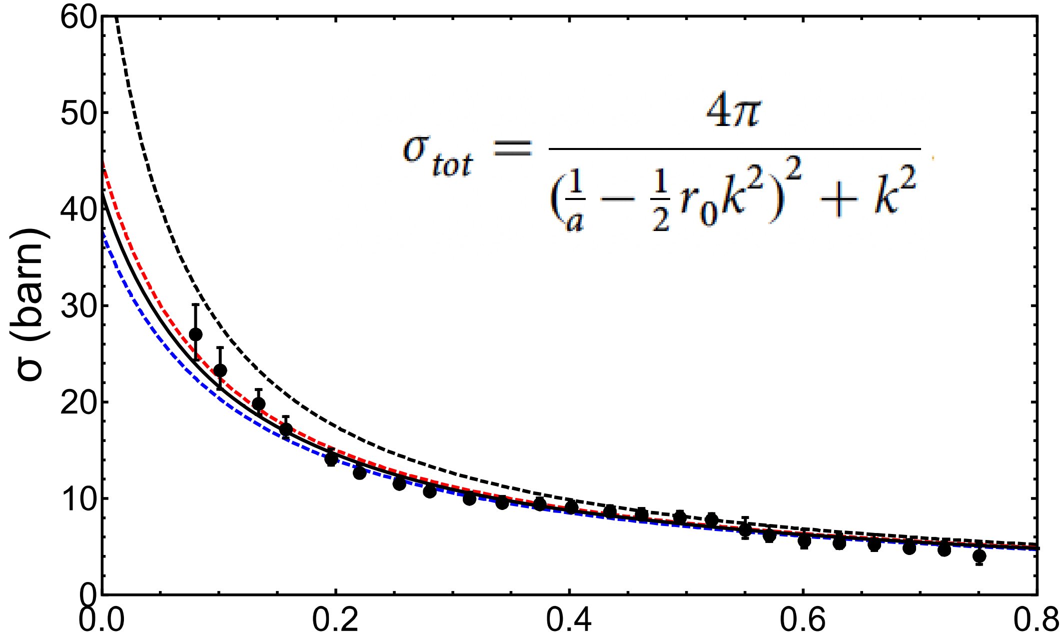

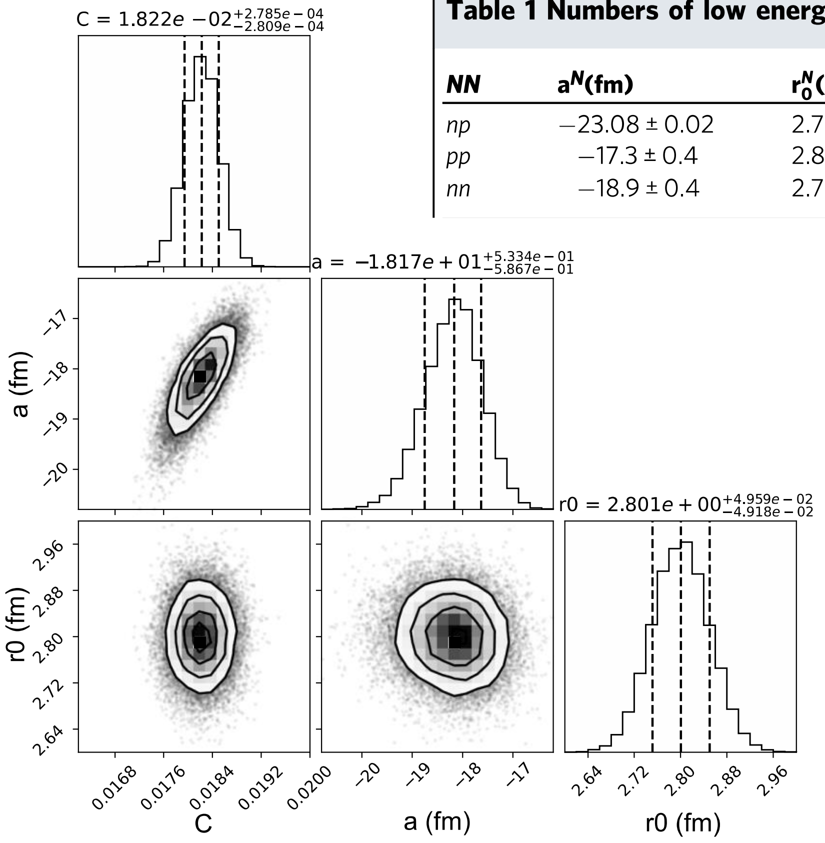

Table 1 Numbers of low energy parameters.

NN	a^N(fm)	r_0^N(fm)	a^{THM}(fm)	r_0^{THM}(fm)
np	−23.08 ± 0.02	2.77 ± 0.05		
pp	−17.3 ± 0.4	2.85 ± 0.04	$-18.17^{+0.53}_{-0.59}$ fm	2.80 ± 0.05 fm
nn	−18.9 ± 0.4	2.75 ± 0.11		

Notice: the NN s-wave phase shift δ contains all short range effects, including the electromagnetic ones. This means that the present analysis of the HOES cross section allows direct access to the short-range p-p interaction as a whole, with its peculiar a_{pp} and r_0 values.

We propose a new paradigm: to assess the charge symmetry breaking of the short-range interaction as a whole, in line with the current understanding that, at a fundamental level, the charge dependence of nuclear forces is due to a difference between the masses of the up and down quark and to electromagnetic interactions among the quarks.

We can exploit universal concepts to better interpret the results: in the universal window the dynamics is largely independent of the details of the interaction. It is dominated by the long-range behavior allowing for a description based on few parameters.

We construct a two-parameter Gaussian NN interaction with fixed range, valid for s-wave in the spin singlet channel

$$V_{NN}(r) = V_0 e^{-r^2/r_G^2} + \frac{e_{NN}^2}{r}$$

with NN ≡ nn, np, pp and $e^2_{pp} = e^2$ and zero otherwise

the Gaussian form selected to represent the short-range interaction is not relevant, other choices are acceptable as well. Very recently a new calculation using the Eckart potential that exactly represents the S-matrix for the NN system in the universal window (S-matrix is equivalent to the effective range expansion up to the second order):

$$V_{Eck}(\beta, R, r) = -2\frac{\hbar^2}{mR^2}\frac{\beta e^{-r/R}}{(1+\beta e^{-r/R})^2}$$

$$a = 4R\frac{\beta}{\beta-1} \qquad r_0 = 2R\frac{\beta+1}{\beta}$$

NN	a^N(fm)	r_0^N(fm)	a^{THM}(fm)	r_0^{THM}(fm)	a^{sr}(fm)	r_0^{sr}(fm)
np	-23.08 ± 0.02	2.77 ± 0.05			-23.74± 0.02	2.80 ± 0.08
pp	-17.3 ± 0.4	2.85 ± 0.04	$-18.17^{+0.53}_{-0.59}$	2.80±0.05	-17.9 ± 0.5	2.85 ± 0.09
nn	-18.9 ± 0.4	2.75 ± 0.11			-18.6 ± 0.4	2.85 ± 0.08

A. Tumino, A Kiewsky et al. Few Body Systems 2025

Bridging fundamental NN symmetries and astrophysics: can precise pp scattering length determinations directly refine solar fusion S-factors and neutrino flux models?

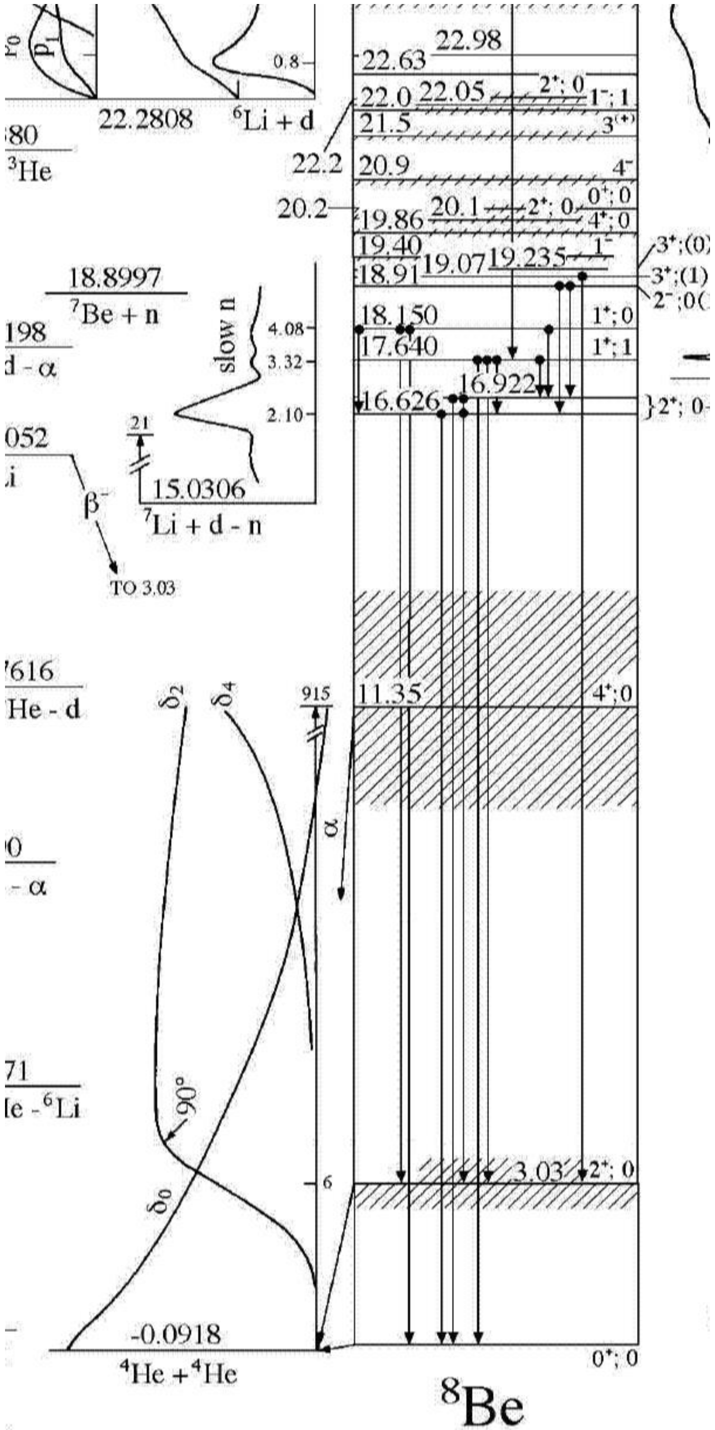

Another topic … moving up with the ^{12}C excitation energy …

…via the ^{6}Li + ^{6}Li → 3α reaction at 3.1 MeV

Upper part of ^{12}C level scheme

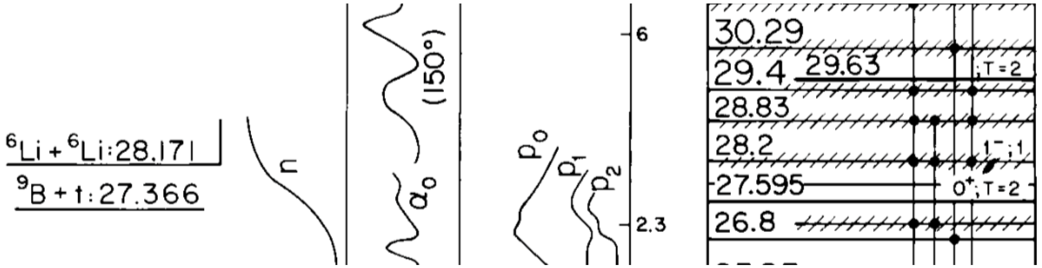

Evidence: events with correlated α's fed by two and even three ^{8}Be in the same event

→ existence of α-trimers (?)

We are at an excitation energy of ^{12}C of about 29.6 MeV (^{6}Li + ^{6}Li threshold: 28.17 MeV; center-of-mass beam energy at half target: 1.4 MeV).

However, energy comes from the Q-value

Event projection onto the Eij (i, j = 1,2,3) relative energy axis:

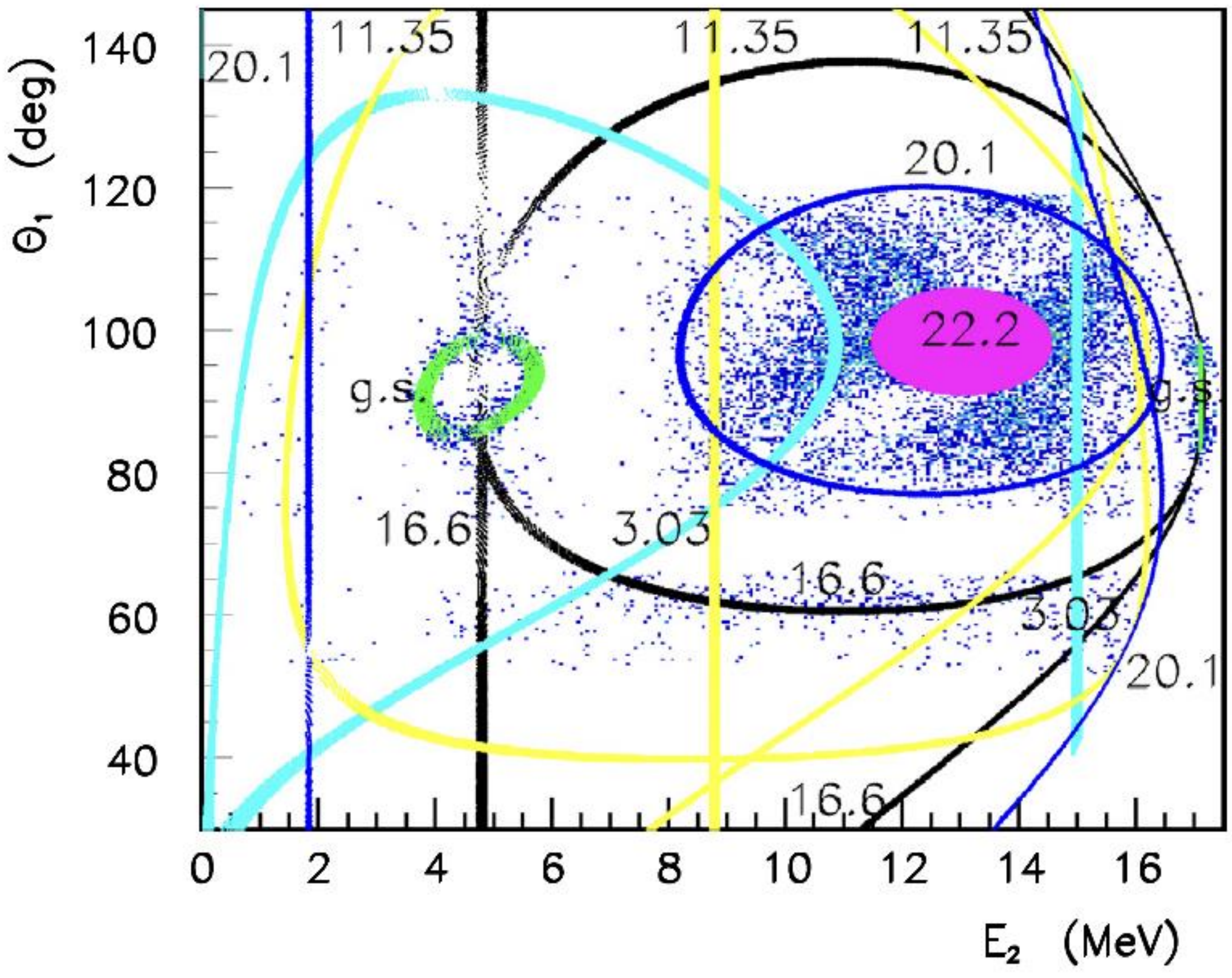

A. Tumino et al. PLB (2015) 59

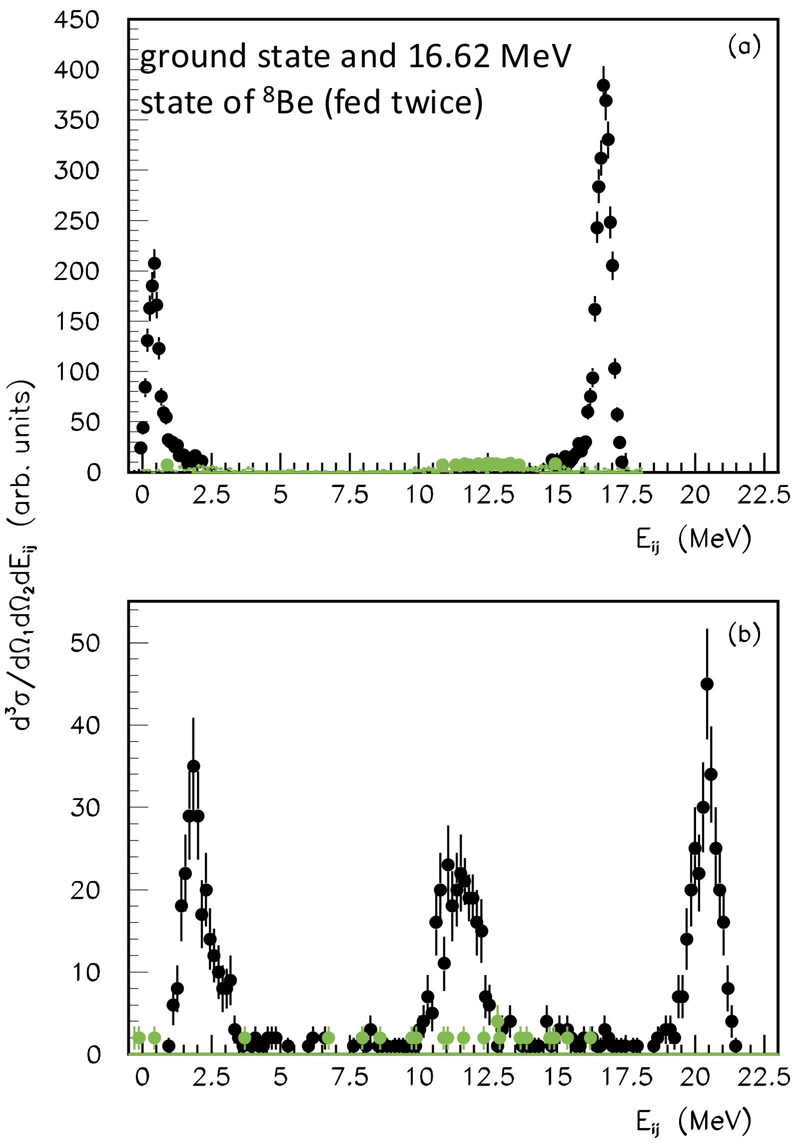

three ^{8}Be states at 20.1, 11.35 and 3.03 MeV, taking advantage of their huge widths

Can this alpha correlation be connected with the Efimov mechanism?

Efimov mechanism: is an effect in the quantum mechanics of few-body systems predicted by Efimov in 1970.

Efimov idea: A system of three particles with resonant two-body interactions may form bound states, the so called Efimov trimers, even when any two of the particles are unable to bind.

First experimental evidences in 2005 in an ultracold atomic systems.
Further proofs …

No clear observation exists yet in nuclei - However several studies in two-neutron halo-nuclei, such as ^{11}Li and ^{22}C

For 12C: the Hoyle state cannot be an Efimov state

Our predictions: Efimov like effects at E_exc ~ 7.45 MeV
Of course the Coulomb repulsion strongly suppresses any 3a correlation, but still potential FSI can have importance for He-burning
…

Efimov has predicted the possibility of existence of trimers in a system of three α-particles, with a maximum radius of attraction of the order of the Bohr radius, $a_C = 1/e^2$, due to the repulsive long-range Coulomb potential.